

## CALCINATION OF ALUMINUM CHLORIDE HEXAHYDRATE (ACH) FOR ALUMINA PRODUCTION: IMPLICATIONS FOR ALUMINA EXTRACTION FROM ALUMINUM RICH FLY ASH (ARFA)

Alumina rich fly ash (ARFA) has been regarded as the alternative to bauxite in China. Hydrochloric acid process could be favored for alumina extraction, necessitating calcination of aluminum chloride hexahydrate (ACH). In this work, the TGA/DSC results of ACH were used to suggest calcination procedures. Two-step calcinations of 200-1000°C and 350-1000°C did not increase the surface area of alumina, by comparison with one step 1000°C calcination, and a slow heating rate could improve the surface area. Calcination temperature was increased from 950 to 1250°C in a step of 50°C, and XRD, XRF, BET and gas pycnometer were used to characterize the alumina from calcinated ACH. Consistent results were obtained by these different techniques, and two groups of impurities were identified and related to alumina purity and surface area. By comparison with clays, it was suggested to remove impurities such as MgO, Na<sub>2</sub>O, K<sub>2</sub>O, P<sub>2</sub>O<sub>5</sub> and SO<sub>3</sub> in hydrochloric acid leaching of ARFA.

*Keywords:* calcination; aluminum chloride hexahydrate; alumina rich fly ash; acid leaching

### 1. Introduction

Over 90% of alumina (Al<sub>2</sub>O<sub>3</sub>) has been consumed to produce aluminum nowadays, one of most useful metals in the world. The main route for its production is Bayer process, which uses bauxite as the alumina resource to produce aluminum hydroxide for decomposition to alumina by calcination. Though bauxite seems to be enough for many years to come, it does not distribute evenly among different countries. Many alumina resources, such as clays and fly ashes, have long been regarded as the alternatives to bauxite, for which some new routes other than Bayer process for alumina extraction are needed [1-3].

Early investigations on the routes for alumina extraction from non-bauxite alumina resources have found that hydrochloric acid leaching was among the best [1,2]. In recent years, there is renewed interest in developing the hydrochloric acid process for alumina extraction [4,5]. New technologies based upon hydrochloric acid process have enabled the environmentally-neutral extraction of smelter-grade alumina (SGA), high-purity alumina (HPA), and high-value elements, including rare earths and rare metals, from a variety of alumina resources [6,7]. In the year 2000, a group of researchers found that the coal in Jungar deposit of Inner Mongolia, China, is enriched with alumina up to 15%, due to the destruction of neighboring bauxite deposits during the Late Paleozoic age [8]. Alumina rich coal (ARC) has been usually burned to generate electricity in power plants, and alumina can get even concentrated in the fly ash. It has been

estimated that 10-30 billion tons of alumina rich fly ash (ARFA) with about 50wt% alumina would be produced [9]. The discovery of ARFA has brought about the hope for alumina independence for China, and one demonstration plant has been commissioned by using the hydrochloric acid leaching [3,8,9].

The key steps for alumina extraction by hydrochloric acid leaching of ARFA could be the production of aluminum chloride hexahydrate (ACH), and the subsequent calcination for alumina. Alternatively, alumina could be produced by costly spray pyrolysis of aluminum chloride solution [10]. ACH has been obtained by crystallization through evaporation, HCl sparging and concentrated hydrochloric impouring of leaching solutions from digested slurry of alumina bearing ores [1,5]. For ACH calcination, early investigations have focused on the identification of phases in the process [11-13]. Because hydrochloric acid leaching would not involve the addition of sodium bearing agents, ACH has been calcinated to produce low-soda alumina [2]. More recently, ACH has been partially decomposed at low temperatures for basic aluminum chloride, which can be dissolved to produce poly(aluminum chloride) [14-16].

Till now, few investigations have been made to produce smelter-grade alumina (SGA) by hydrochloric acid leaching of ARFA. Modern SGA necessitates low impurities and high surface area. Low impurities help to increase the efficiency of electrolysis, decrease energy consumption and unnecessary pollutions. High surface area would be beneficial for HF adsorption by alumina for its return to the smelter electrolyte, which is a green

\* NATIONAL INSTITUTE OF CLEAN-AND-LOW-CARBON ENERGY, P. O. BOX 001 SHENHUA NICE, XIAOTANGSHAN FUTURE SCIENCE & TECHNOLOGY CITY, CHANGPING DISTRICT, BEIJING 102211, PR CHINA

# Corresponding author: zhaolijun@nicenergy.com

process adopted widely by the industry. This work represents an effort to evaluate the alumina from calcinated ACH, which has been produced by hydrochloric leaching of ARFA.

## 2. Experimental

By following the similar procedures adopted previously in the alumina extraction from clays [1], and with Ca removal by resin, the ACH has been prepared by the ARFA from one of coal-fired power plants of Inner Mongolia, China. The ARFA was found to have a BET surface area of 2.6 m<sup>2</sup>/g and a true density 2.44 g/cm<sup>3</sup>. The chemical compositions of ARFA are given in Table 1 in form of stable oxides of elements, and the chemical compositions of measurable impurities in ACH are also given in Table 2 in form of stable oxides.

Chemical compositions (wt%) of ARFA in form of stable oxides of elements

SiO <sub>2</sub>	TiO <sub>2</sub>	Al <sub>2</sub> O <sub>3</sub>	TFe <sub>2</sub> O <sub>3</sub>	MnO	MgO	CaO	Na <sub>2</sub> O	K <sub>2</sub> O	P <sub>2</sub> O <sub>5</sub>	SO <sub>3</sub>	LOI	Total
40.01	1.57	50.71	1.76	0.02	0.47	2.85	0.12	0.50	0.17	0.22	1.41	99.81

TABLE 2

Chemical compositions (wt%) of impurities in ACH in form of stable oxides

SiO <sub>2</sub>	Fe <sub>2</sub> O <sub>3</sub>	MgO	CaO	Na <sub>2</sub> O	K <sub>2</sub> O	P <sub>2</sub> O <sub>5</sub>	SO <sub>3</sub>
0.011	0.003	0.118	0.006	0.215	0.074	0.151	0.183

Thermal decomposition analysis of the ACH was performed by TGA/DSC (NETZSCH STA 449F3), according to which the calcination procedures were proposed to test the effects of two-step calcination, heating rate and calcination temperature on physicochemical properties of alumina. An ACH sample of 30.0g calcinated at 1000°C for one hour was used as the benchmark, which was heated at a rate of 5.55°C/min from the ambient temperature.

**Two-step Calcination Effect:** Two-step calcinations were carried out by setting the first calcination temperature at 200 or 350°C for one hour by heating the ACH from the ambient temperature, and the second calcination temperature at 1000°C for one hour by heating at a rate of 5.55°C/min. **Heating Rate Effect:** The ACH was calcinated at 1000°C for one hour, by heating the sample at a rate of 2.77°C/min from the ambient temperature, or by placing the sample in a preheated 1000°C muffle furnace, allowing for the heating rate effect to be identified. **Calcination Temperature Effect:** The calcination temperature was increased in a step of 50°C from 950 to 1250°C, which is the reasonable range for alumina calcination, to evaluate the calcination temperature effect at a heating rate of 5.55°C/min.

All the calcinated samples were analyzed by the XRF (ZSX Primus II) for chemical compositions, by the BET analyzer (TriStar 3000) for surface areas, by the XRD (RINT 2000) for phase changes, and by the gas pycnometer (AccuPyc II 1340) for true densities.

## 3. Results and discussion

### 3.1. Thermal decomposition analysis of ACH by TGA/DSC measurement

The TGA/DSC measurement has been made for the ACH prepared from ARFA, as given in Figure 1. For the left y axis for ACH mass with increasing the temperature, noticeable decomposition of ACH starts from about 110°C, proceeds at the highest rate at around 200°C, and almost finalizes at around 350°C, which is similar to previous observations [2]. For the right y axis for DSC with increasing the temperature, the negative peak occurs at around 215°C. This observation is reasonable because loss of mass is relevant to DSC, but not exactly the same. With increasing further the temperature, the calcinated mass becomes almost constant, but the DSC remains stable only up to about 500°C, and a positive peak at 875°C indicates the phase change by releasing heat, probably from amorphous to crystalline state. The gentle slope of decline starting from around 500°C might be partially ascribed to the drift of DSC baseline with the increase

of temperature, or possibly the heat-absorbing property of the calcinated alumina from ACH, collecting energy for the later phase transformation.

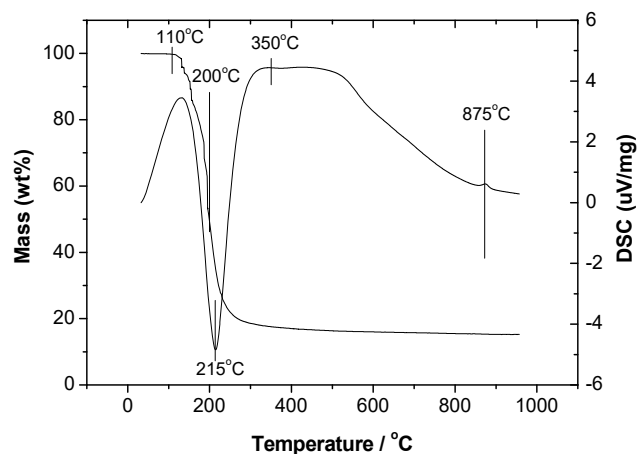


Fig. 1. TGA/DSC measurement of ACH prepared from ARFA

Previous investigations of ACH thermal decomposition have concentrated in particular on two ranges, i.e., the low temperature range from the ambient to 270°C, and the high temperature range from 400 to 1400°C [2,11-16]. In the low temperatures, the decomposition kinetics has been investigated for the production of basic chlorides [14]. In the high temperatures, the identification of phase changes for alumina was the main purpose [11]. It has been suspected that the calcination step could affect the physicochemical properties of alumina from calcinated ACH. Calcination at 200°C produced the basic chlorides [14-16], and above 300°C but prior to the phase change at 875°C, amorphous alumina was formed from calcination, according to

Figure 1. Therefore, 200 and 350°C has been selected as the first step calcination temperatures in the two-step calcinations as detailed in the Experimental section. In addition, heating rate and calcination temperature could also affect the alumina properties [14-16], and the effects will be discussed in the following.

### 3.2. Two-step calcination effect on physicochemical properties of alumina

For two-step calcinations of 200-1000°C and 350-1000°C, the XRD spectra of calcinated ACH are given in Figure 2. In Figure 2a, the calcinated ACH at 200°C is characterized by many sharp peaks, which can be assigned to the chloraluminite (PDF: 73-0301). Calcination at 200°C causes a mass loss of about 30wt%, which corresponds to an ACH decomposition of 40wt% [14], therefore, the XRD spectra are much like those for ACH. In Figure 2b, the calcinated ACH at 350°C is transformed to the water-free amorphous state, and some small peaks above the broad band can be ascribed to AlO (PDF: 75-0278), which has been observed either in aluminum oxide suspension [17] or as the corrosion product [18]. In both cases, when the first step samples are further calcinated at 1000°C for one hour, the final products have been consistently identified as active alumina (PDF: 74-2206), which has a purity of 95.2-95.4wt%, much lower than the SGA purity of above 98.6wt% (YS/T 803-2012).

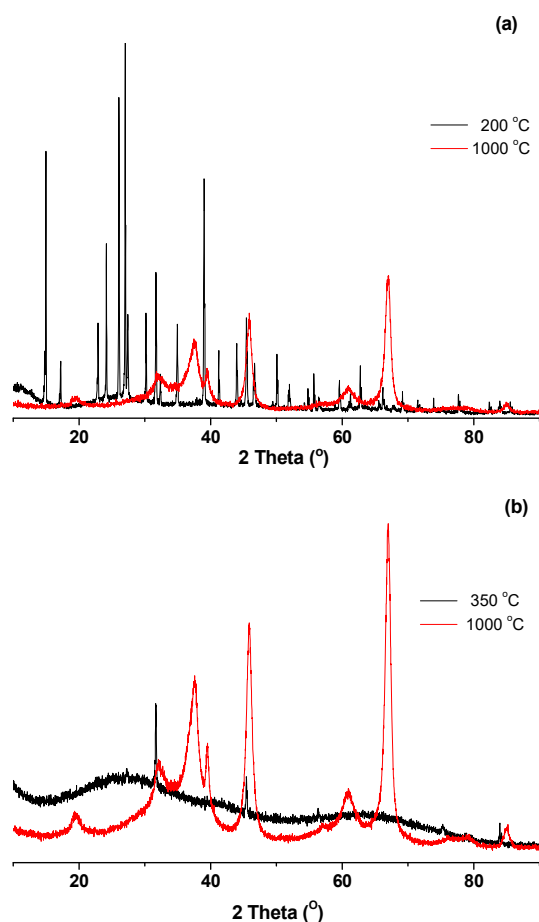


Fig. 2. XRD spectra of calcinated ACH in two-step calcinations of 200-1000°C (a) and 350-1000°C (b)

The BET surface areas of calcinated ACH are 51.2 and 55.8 m<sup>2</sup>/g for two-step calcinations of 200-1000°C and 350-1000°C. By contrast, much higher BET surface area of 66.5 m<sup>2</sup>/g has been obtained from one step 1000°C calcination. It has been recognized that ACH hydrolysis occurs in the calcination process [19]. In the first step calcinations of 200 and 350°C, HCl and water evaporations would be retarded due to rapid hydrolysis, causing detrimental effect on the structures of calcinated ACH, which cannot be recovered even with a second step 1000°C calcination. The true densities of calcinated ACH are 3.46, 3.42, 3.48 g/cm<sup>3</sup> for two-step calcinations of 200-1000°C, 350-1000°C, and one step 1000°C calcination. The small differences between true densities are reasonable, because the phases are the same.

### 3.3. Heating rate effect on physicochemical properties of alumina

To slow the calcination, the heating rate for calcination at 1000°C was decreased by half from 5.55 to 2.77°C/min, the BET surface area was 68.0 m<sup>2</sup>/g, and the true density was 3.40 g/cm<sup>3</sup>. To speed up the heating, the muffle furnace was preheated to 1000°C, the ACH was settled for one hour calcination, the BET surface area was 55.8 m<sup>2</sup>/g, and the true density was 3.49 g/cm<sup>3</sup>. As a result, for 1000°C calcination heating from the ambient temperature, it seems that a slow heating rate would be very favorable for high BET surface area of alumina from calcinated ACH. Since decreasing the heating rate from 5.55 to 2.77°C/min was observed to marginally increase the BET surface area from 66.5 to 68.0 m<sup>2</sup>/g, the heating rate of 5.55°C/min was generally adopted in this work. The small difference between the two true densities may indicate that similar phases occur in the calcinated ACH.

The ACH was then calcinated at 1050°C, the BET surface area decreased to 59.8 m<sup>2</sup>/g, and the true density increased to 3.52 g/cm<sup>3</sup>. In Figure 3, the XRD spectra for 1000°C calcinations

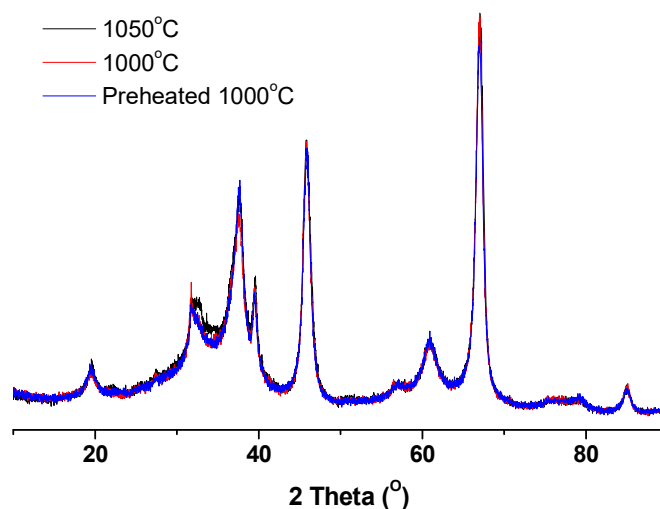


Fig. 3. XRD spectra of alumina from calcinated ACH at 1050°C and 1000°C by heating from ambient temperature, and by placing ACH in a preheated 1000°C muffle furnace

at different heating rates and for 1050°C calcination are displayed for comparisons. Despite the differences in BET surface areas and true densities as discussed above, the XRD spectra for three samples are almost the same, and the main phase is active alumina (PDF: 74-2206). At the same time, the alumina from calcinated ACH at 1050°C was purified to 96.3wt%.

### 3.4. Calcination temperature effect on physicochemical properties of alumina

Since calcination temperature was found to affect the BET surface area, the true density, and the purity of alumina from calcinated ACH in Section 3.3, it was further varied from 950 to 1250°C in a step of 50°C, the reasonable temperature range for alumina calcination.

The XRD spectra of the alumina from calcinated ACH are given in Figure 4. It is apparent that the phase change from active alumina (PDF: 74-2206) to corundum (PDF: 83-2080) occurs from 1150-1200°C, but a close look as given in the enlarged window in the upper right part of Figure 4 indicates that some spectral changes appear even from 1100°C.

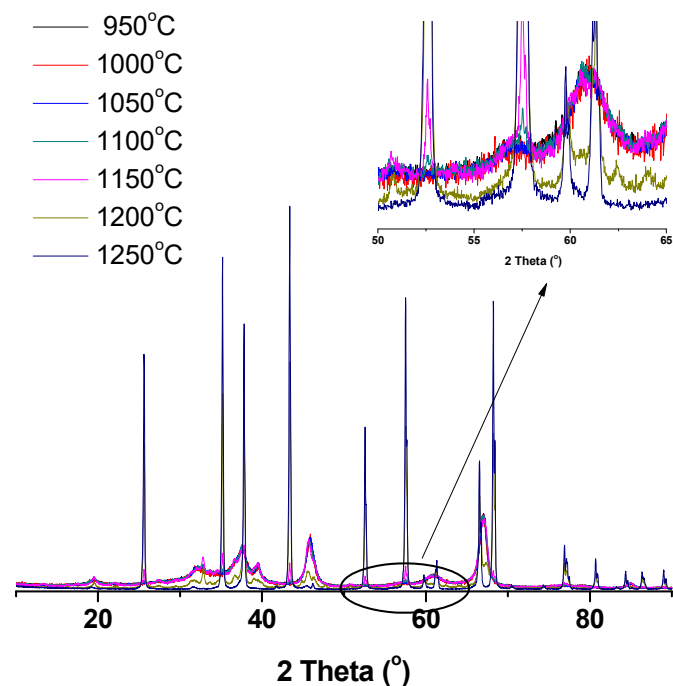


Fig. 4. XRD spectra of alumina from calcinated ACH in a step of 50°C from 950 to 1250°C. Enlarged window indicates some phase changes at about 1100°C

The true densities and impurities of alumina from calcinated ACH are given in Figure 5 as a function of the calcination temperature. Prior to 1100°C, the true density increases slightly from 3.40 to 3.54, corresponding to active alumina, and from 1100 to 1250°C, it starts to ascend markedly and finally reaches 4.12, corresponding to corundum [20]. This trend is in good agreement with the above XRD observation of the transformation from active alumina to corundum in Figure 4.

For the impurities according to Figure 5, they can be classified into two groups with increasing the calcination temperature, i.e., those with basically constant fractions (Group I), such as CaO, MgO, SiO<sub>2</sub> and Fe<sub>2</sub>O<sub>3</sub>, and those with the decreasing fractions (Group II), such as Cl, Na<sub>2</sub>O, K<sub>2</sub>O, P<sub>2</sub>O<sub>5</sub> and SO<sub>3</sub>. For Group I impurities, CaO, SiO<sub>2</sub> and Fe<sub>2</sub>O<sub>3</sub> are below 0.1-0.2wt%, and MgO has a constant value of 0.5-0.6wt%, which impacts seriously on alumina purity. For Group II impurities, the temperature 1100°C seems to be a turning point, which coincides with the occurrence of phase changes in the XRD spectra in Figure 4. Since Group I impurities do not change much in the calcination process, Group II impurities could possibly account for the most variations, not only the phase changes, but the physicochemical properties of the alumina from calcinated ACH.

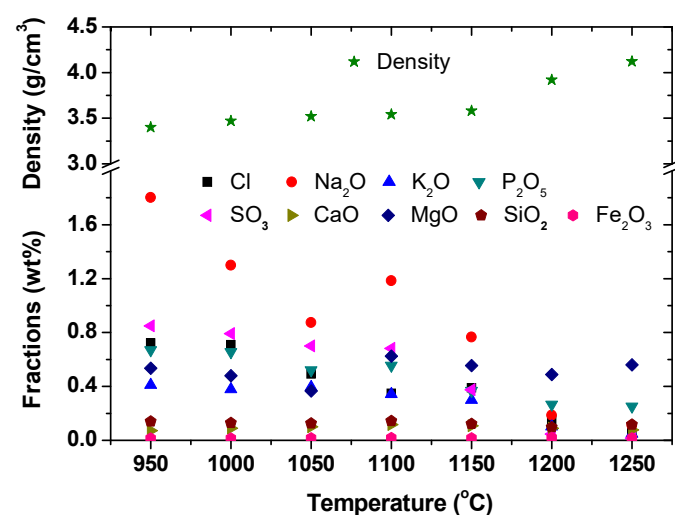


Fig. 5. True densities ( $\text{g}/\text{cm}^3$ ) and impurities fractions (wt%) in form of stable oxides, except for Cl, of alumina from calcinated ACH in a step of 50°C from 950 to 1250°C

In Figure 6, Group II impurities could be related to the BET surface areas of alumina from calcinated ACH. Prior to the calcination temperature 1100°C, the fractions of Group II impurities decrease in gentle slopes, but with passing through the 1100°C, the slopes become much sharper. The BET surface areas of alumina from calcinated ACH follow similar patterns with the increase of calcination temperature in a step of 50°C from 950 to 1250°C. The BET surface areas are weakly affected before 1100°C, after which the BET surface area decreases rapidly with the increase of calcination temperature. There are no direct evidences on the roles of Group II impurities on the BET surface area of alumina from calcinated ACH. But it could be that, with the phase change from active alumina (with high BET surface area) to corundum (with low BET surface area) [2,11-13], Group II impurities Cl, Na<sub>2</sub>O, K<sub>2</sub>O, P<sub>2</sub>O<sub>5</sub> and SO<sub>3</sub> would be released due to structure rearrangements with increasing the temperature, and the BET surface area would decrease accordingly as corundum is accumulated. By comparison, Group I impurities CaO, MgO, SiO<sub>2</sub> and Fe<sub>2</sub>O<sub>3</sub> are much less volatile in small amounts.

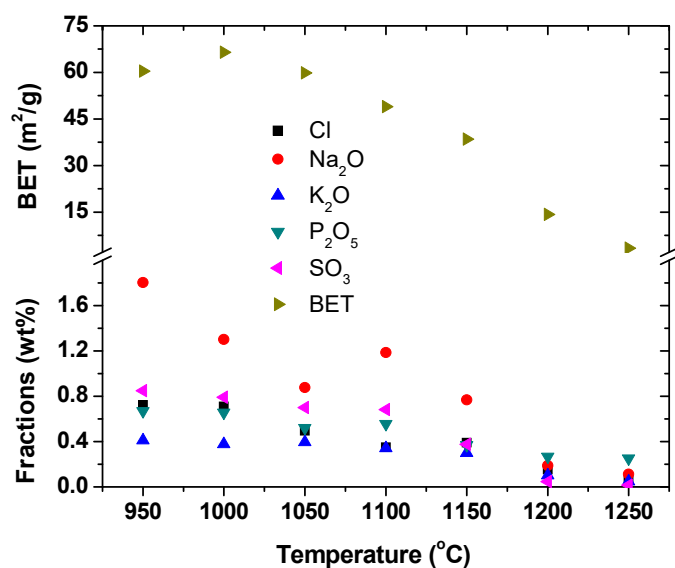


Fig. 6. Fractions of Group II impurities (wt%) in relation to the BET surface areas of alumina from calcinated ACH in a step of 50°C from 950 to 1250°C

In Figure 7, Group II impurities could also be related to the purity of alumina from calcinated ACH. Since the fractions of Group I impurities do not change much in the calcination process, the alumina fractions naturally follow a reverse pattern by comparison with Group II impurities. With Group II impurities being rapidly reduced after the calcination temperature 1100°C, the alumina purity increases in a reverse way. Nevertheless, the SGA necessitates a high purity of above 98.6wt% (YS/T 803-2012), which can only be achieved by calcination at temperatures above 1200°C, according to Figure 7.

### 3.5. Implications for alumina extraction by hydrochloric acid leaching of ARFA

By comparison with the clays used for alumina extraction by hydrochloric acid process [1], many impurities in ARFA can be in excess in 1-2 orders of magnitude. Moreover, the impurities in ARFA could be easily attacked by hydrochloric acid. As a result, the alumina from calcinated ACH in this work has high levels of impurities, which need to be removed.

It can be seen that impurities are hindering the production of alumina with high purity and surface area, as required for modern alumina electrolysis. Alumina extraction by the current hydrochloric acid leaching has successfully reduced Group I impurities to acceptable levels, except for MgO. Increasing the calcination temperature, especially above 1100°C, can be effective in removing Group II impurities, but decreases the surface area.

The sample of sandy alumina (i.e., SGA) by Bayer process was collected from one production line of modern alumina electrolysis in China. Sandy alumina is characterized by a purity of 99.1wt%, a BET surface area of 90.2 m<sup>2</sup>/g, and a true density of 3.43g/cm<sup>3</sup>. The XRD spectra of sandy alumina are given in Figure 8, as well as the alumina from calcinated ACH. Due to light

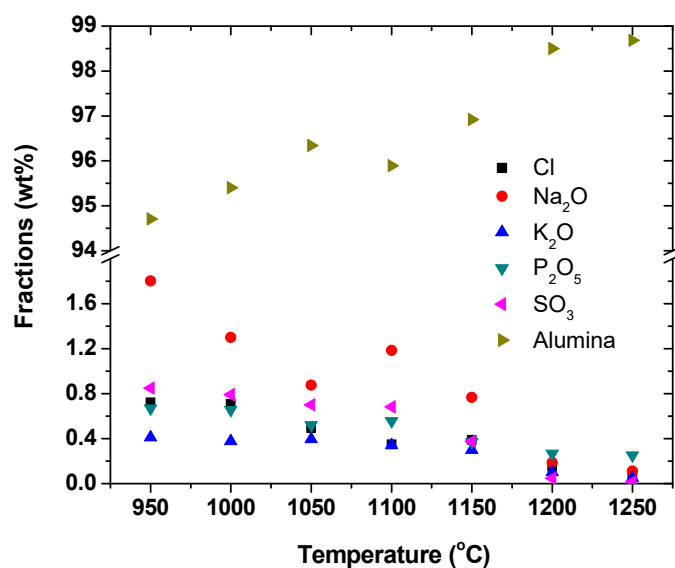


Fig. 7. Fractions of Group II impurities (wt%) in relation to the purity of alumina from calcinated ACH in a step of 50°C from 950 to 1250°C

scattering, the XRD spectra for sandy alumina present a slope toward the low 2 Theta. Despite the significant difference in BET surface areas between sandy alumina (90.2 m<sup>2</sup>/g) and the alumina (49.0-59.8 m<sup>2</sup>/g) from calcinated ACH at 1050-1100°C, according to Figure 8, sandy alumina resembles nicely the alumina from calcinated ACH at 1050-1100°C. Moreover, the true density of 3.43 g/cm<sup>3</sup> for sandy alumina is also close to the true densities of 3.52-3.54 g/cm<sup>3</sup> for the alumina from calcinated ACH at 1050-1100°C. Therefore, increasing the calcination temperature not only decreases the surface area, but causes harmful phase changes in the alumina from calcinated ACH.

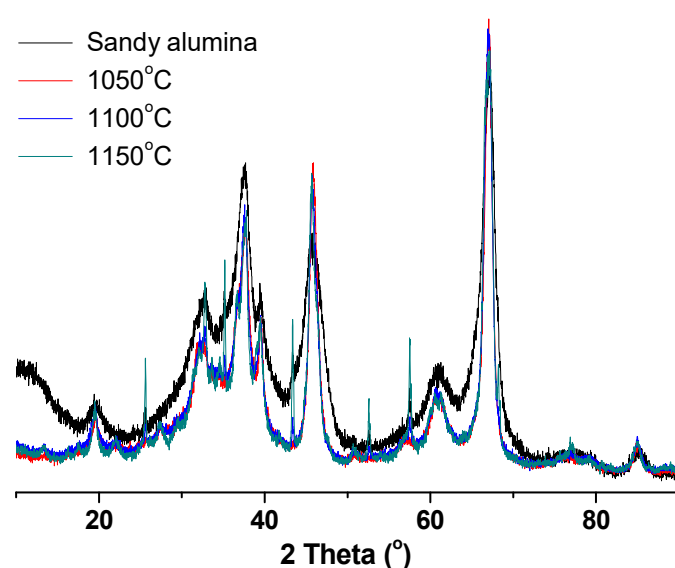


Fig. 8. XRD spectra of sandy alumina by Bayer process and alumina from calcinated ACH at temperatures of 1050, 1100 and 1150°C

The only method left for SGA production from calcinated ACH seems to remove more impurities in hydrochloric acid

leaching of ARFA, especially, Group I impurities like MgO, and Group II impurities like Na<sub>2</sub>O, K<sub>2</sub>O, P<sub>2</sub>O<sub>5</sub> and SO<sub>3</sub>. Removing impurities definitely adds to the cost of hydrochloric acid leaching, but the good news is that low impurities decrease the calcination temperature by at least 100-150°C, which is the most energy-intensive process.

#### 4. Conclusion

In recent years, alumina rich coal (ARC) has been found in Jungar deposit, and after being burned for power generation, the resulting alumina rich fly ash (ARFA) has been regarded as the promising alternative alumina resource and received much attention in China, which is facing the shortage of bauxite. Hydrochloric acid process could provide an economical way for alumina extraction from ARFA, and calcination of aluminum chloride hexahydrate (ACH) is the key step for alumina production. Modern smelter-grade alumina (SGA) necessitates low impurities and high BET surface area for efficiency and pollution reduction.

TGA/DSC has been used to study the ACH prepared from hydrochloric acid leaching of ARFA, revealing the thermal decomposition process and phase changes, and the calcination procedures were suggested. Two-step calcinations of 200-1000°C and 350-1000°C did not increase the BET surface area of alumina from calcinated ACH, by comparison with one step 1000°C calcination. A slow heating rate could improve the surface area, but the calcination temperature was the major factor. The calcination temperature was then increased from 950 to 1250°C in a step of 50°C, and XRD, XRF, BET and gas pycnometer were used to systematically characterize the alumina from calcinated ACH. The phase change from active alumina to corundum was observed to occur at 1100°C, which is in good agreement with the trend of true density, and two groups of impurities were identified. Group I impurities like CaO, MgO, SiO<sub>2</sub> and Fe<sub>2</sub>O<sub>3</sub> were characterized by relative constant fractions in alumina from calcinated ACH, whereas Group II impurities like Cl, Na<sub>2</sub>O, K<sub>2</sub>O, P<sub>2</sub>O<sub>5</sub> and SO<sub>3</sub> decreased in fractions with the increase of calcination temperatures, especially after 1100°C. The phase, true density, and Group II impurities could be related to the physicochemical properties of alumina, such as alumina purity and surface area. Due to the high levels of impurities in ARFA, it has been suggested to remove more impurities such as MgO, Na<sub>2</sub>O, K<sub>2</sub>O, P<sub>2</sub>O<sub>5</sub> and SO<sub>3</sub> in the hydrochloric acid leaching of ARFA for SGA production.

#### Acknowledgement

This work was financially supported by the National Hi-tech Research and Development Program of China (863 Program, 2012AA06A115), and the China Shenhua Group Science and Technology Innovation Foundation project (ST930013SH05).

#### REFERENCES

- [1] J.A. Elsele, D.J. Bauer, D.E. Shanks, *Ind. Eng. Chem. Prod. Res. Dev.* **22** (1), 105-110 (1983).
- [2] K.Y. Park, J. Jeong, *Ind. Eng. Chem. Res.* **35** (11), 4379-4385 (1996).
- [3] Z.T. Yao, M.S. Xia, P.K. Sarker, T. Chen T, *Fuel* **120**, 74-85 (2014).
- [4] M.S.R. Sarker, M.Z. Alam, M.R. Qadir, M.A. Gafur, M. Moniruzzaman, *Int. J. Miner. Metall. Mater.* **22** (4), 429-436 (2015).
- [5] Y. Guo, H. Lv, X. Yang, F. Cheng, *Sep. Purif. Technol.* **151**, 177-183 (2015).
- [6] K. Binnemans, P.T. Jones, B. Blanpain, T.V. Gerven, Y. Pontikes, *J. Clean. Prod.* **99**, 17-38 (2015).
- [7] A.N. Løvik, E. Restrepo, D.B. Müller, *Environ. Sci. Technol.* **49** (9), 5704-5712 (2015).
- [8] V.V. Seredin, *Int. J. Coal Geo.* **90-91**, 1-3 (2012).
- [9] L. Zhao, H. Xiao, B. Wang, Q. Sun, *J. Chem.* 2016, article ID 8695890, 10 pages (2016).
- [10] G. Lü, T. Zhang, L. Wang, S. Ma, Z. Dou, Y. Liu, *J. Cent. South Univ.* **21** (12), 4450-4455 (2014).
- [11] T. Sato, *Netsu Sokutei.* **13** (3), 113-122 (1986).
- [12] D. Petzold, R. Naumann, *J. Therm. Anal.* **20** (1), 71-86 (1981).
- [13] R. Naumann, D. Petzold, F. Paulik, J. Paulik, *J. Therm. Anal.* **15** (1), 47-53 (1979).
- [14] M. Hartman, O. Trnka, O. Šolcová, *Ind. Eng. Chem. Res.* **44** (17), 6591-6598 (2005).
- [15] K.Y. Park, J.-K. Kim, J. Jeong, Y.Y. Choi, *Ind. Eng. Chem. Res.* **36** (7), 2646-2650 (1997).
- [16] K.Y. Park, Y.-W. Park, S.-H. Youn, S.-Y. Choi, *Ind. Eng. Chem. Res.* **39** (11), 4173-4177 (2000).
- [17] C.S. Sen, B. Santanu, *J. Metall. Mater. Sci.* **53** (4), 355-367 (2011).
- [18] D. Thirumalaikumarasamy, K. Shanmugam, V. Balasubramanian, *J. Asian Ceram. Soc.* **2** (4), 403-415 (2014).
- [19] J. Saukkoriipi, Theoretical study of the hydrolysis of aluminum complexes. PhD Dissertation, University of Oulu, Oulu, 2010.
- [20] K. Wefers, C. Misra, *Oxides and hydroxides of aluminum*, Technical Paper No. 19 Revised, Aluminum Company of America, 1987.